A Computational Study of Drug-DNA Interactions

SUMMARY OF THE THESIS

SUBMITTED FOR THE AWARD OF THE DEGREE OF

Doctor of Philosophy

in

Applied Physics

by

Anwesh Pandey

(Enrollment No. - 074/14)

Under the supervision of

Dr. Anil Kumar Yadav

Department of Applied Physics

School for Physical Sciences

Babasaheb Bhimrao Ambedkar University

Lucknow-226025, U.P., India

2020

A Computational Study of Drug-DNA Interactions

The research work carried out in this thesis deals with drug–DNA interactions, their types and applications of elaborate computational techniques to study these interactions and provide underlying explanations for binding of molecules that hold some potential pharmaceutical interest. The thesis consists of seven chapters. Summary of each chapter is given as under.

Chapter-1: Introduction

DNA is a crucial biological target for many anticancer, antiviral, antibacterial and antimicrobial agents in the field of pharmacology and computer aided drug design. Many of these prominent molecules are already in usage whereas still a huge are under various stages of clinical trials. Protein synthesis involving biomolecular processes, such as, transcription and replication are the responsible key parameters for such importance. Transcription involves fetching of genetic codes from DNA to RNA and to direct synthesis of proteins; commonly known as the central dogma of molecular biology. Replication, however involves the DNA to reconstruct and yield two identical strands. DNA starts these processes only after receiving the signal which is usually in the form of regulatory protein to a specific region of DNA.

The main aim of such computer aided and experimental studies is to mimic the production of this regulatory protein by a drug molecule (mainly containing heterocyclic aromatic rings), and hence the functions of DNA can be artificially modulated, inhibited or activated by this small molecule to cure or control a disease

even a particular diseased part of the DNA. The ability of compounds to bind themselves to DNA sequences and interfere with DNA topoisomerases or with the transcription factors has played a crucial role in understanding the mechanism of drug action and many DNA regulated biological activities. Activity of drugs for the treatment of genetic disorders, cancers, bacterial and other microbial infections depends upon their binding modes with DNA. Thus, studies of interaction of drugs with DNA is very interesting and efficient not only to learn the mechanism of interactions but also for designing new and potent drugs.

Although the in-depth information regarding the mechanism of drug-DNA interaction is still unknown, it is necessary to explore more simple methods for investigating their interaction mechanism. The efforts made in the current research work focuses on the computational modelling methods which are used to investigate the molecular basis for drug-DNA recognition and in understanding the roles of hydrogen interactions and factors affecting the stability of drug-DNA complexes. Thus, the investigations on drug-DNA interactions could be very helpful to discover new and advanced drug candidates having minimal side effects. Binding of drugs with DNA occurs through two key modes, viz., groove binding and intercalation. Groove binding owes to binding of drugs in either major or minor grooves of the DNA whereas intercalation involves insertion of planar molecules in between DNA base pairs without damaging the topological double helical structure of the DNA. However, **figure 1** represents a flow chart that easily depicts the modes of DNA binding:

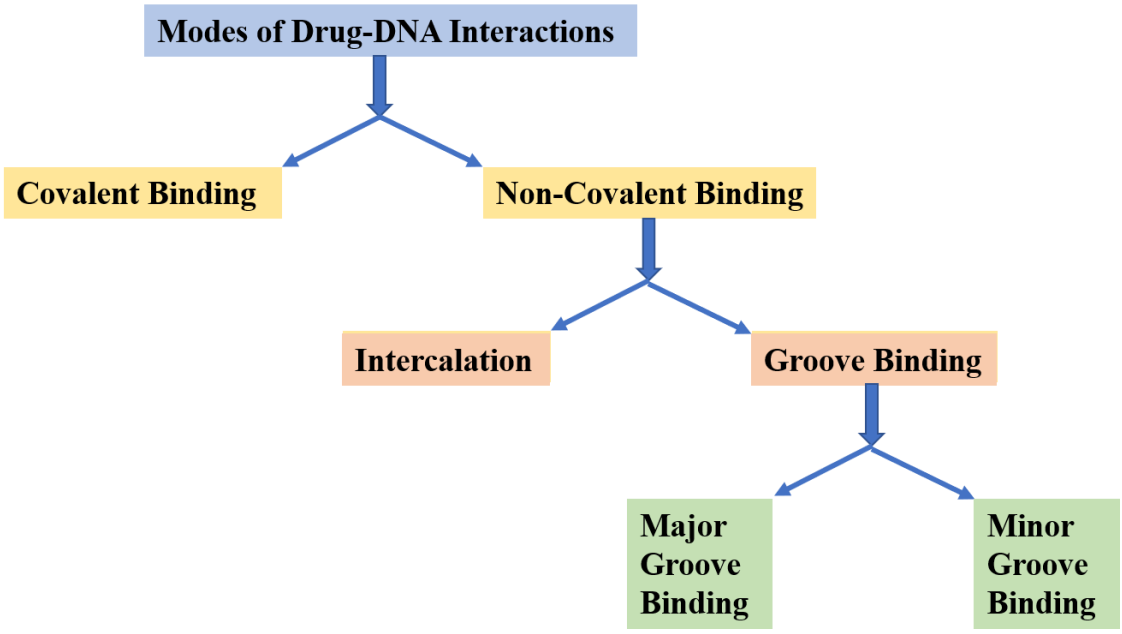

Figure 1: Different modes of drug-DNA interactions

There are various computational experimental and computational (molecular modelling) tools used in the studies of drug-DNA interactions such as, UV-visible spectroscopy, Fluorescence spectroscopy, Circular Dichroism, Viscosity measurements, isothermal titration calorimetry, etc., and some common molecular modelling techniques are molecular docking, molecular dynamics simulations, free energy (thermodynamic) calculations and QM & QM/MM calculations incorporating DFT for better and accurate results and for modelling reaction mechanisms involving drug and DNA; as illustrated in **figure 2**.

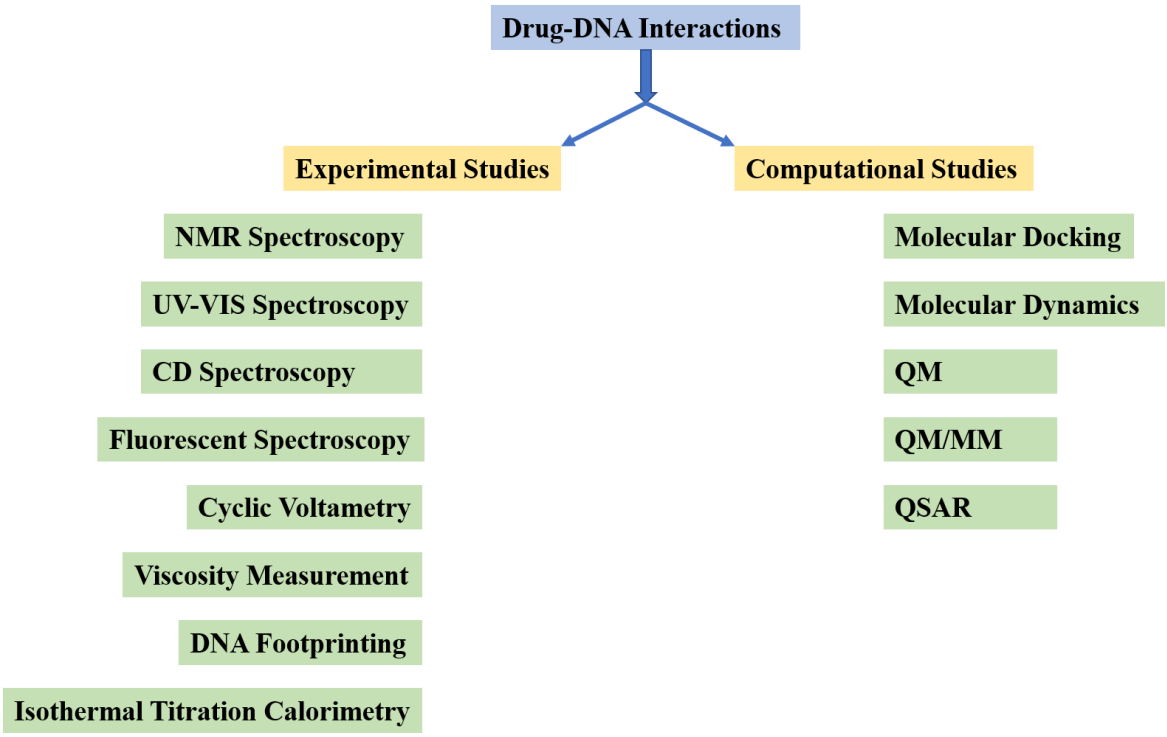

Figure 2: Different methods used to study drug-DNA interactions

Further, molecular modelling methods are able to identify and define crucial details about molecular interactions using high quality molecular graphics tools. We can therefore say that, computer modelling of such biological systems has risen as a powerful tool for complementing experimental investigations by providing theoretical validations. Mere visualization of the obtained experimental data through 3D models cannot just clarify startling outcomes and hence regularly brings up new issues, which influences future research. Therefore, modelling tools such as, molecular docking, molecular dynamics simulations, MMPBSA/MMGBSA calculations, QSAR, virtual screening and QM/MM are the important computational methods which can be used to explore the binding of drug with DNA with desired precisions.

Chapter-2: Methodology

Geometry optimization of studied drug molecules has been carried out using Gaussian 09 at B3LYP/6-31G** level. After geometry optimization molecular docking was performed using AUTODOCK and the best pose was analyzed. MD simulations of the selected docked poses were performed using GROMACS or AMBER. In MD simulation, the complex is put into the water box and relaxed by a series of constrained energy minimization and MM runs at the MM level. After equilibration the system is subjected to a classical MD production runs and the binding energy between drug and DNA was calculated using MMPBSA/MMGBSA method. Snapshots obtained from the MD simulation are taken as starting geometries for the QM/MM calculations. The QM/MM calculations were performed with two-level ONIOM method within the Gaussian 09 program suite (**Figure 3**). DFT method along with basis set 6-31G (d, p) is used for the high layer and AMBER force field for the low layer and all the water molecules are freezed. Geometry optimization of above system was performed and the energy of the high or QM region is calculated. Now, the co-ordinate of QM region from the above optimized system is extracted, which further subjected for geometry optimization and the single point energy calculations of QM region in gas phase using same method. The interaction energy between the DNA and drug molecule is calculated with the help of formula:

$$\Delta E_{IE} = E_{QM(gp)} - E_{QM(pp)} \quad (1)$$

Where,

ΔE_{IE} is the interaction energy between drug and the DNA,

$E_{QM(pp)}$ is the energy of QM region in nucleic acid phase,

$E_{QM(gp)}$ is the energy of QM region in the gas phase.

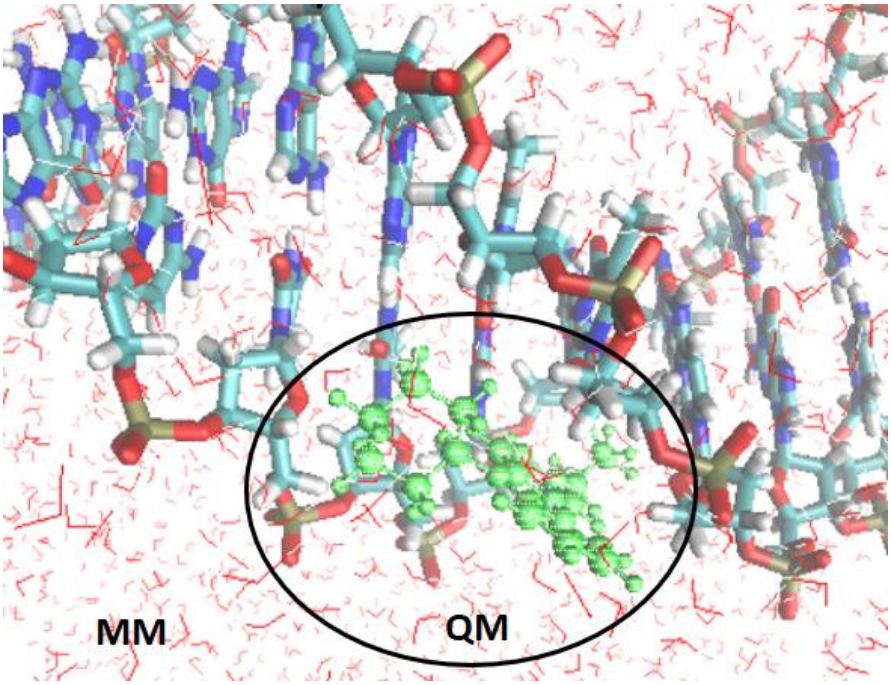

Figure 3: Figure representing a two layered QM/MM (ONIOM) Scheme

Chapter-3: Unveiling the Interactions of Some DNA Minor Groove Binders through Molecular Docking Calculations

In this chapter, two different class of compounds, 2,5-bis(4-amidinophenyl) furan & its derivatives (class 1) and carbazoles & its analogs (class 2) having anti-microbial activity were considered for docking studies. The crystal structures of the selected DNA sequences (1BNA, 1DNE, 1QSX, 1RMX, 195D, 2MNB, 2MNE, 4AH0) were downloaded from Protein Data Bank. These two classes of drugs were then subjected to geometry optimization using Gaussian 09 at B3LYP/6-31G** level. Molecular docking calculations were performed using Autodock4. **Figure 4** & **figure**

5 represent the optimized geometries for class-1 and class-2 compounds, respectively. Whereas, **table 1** and **table 2** represent the obtained docking binding energy.

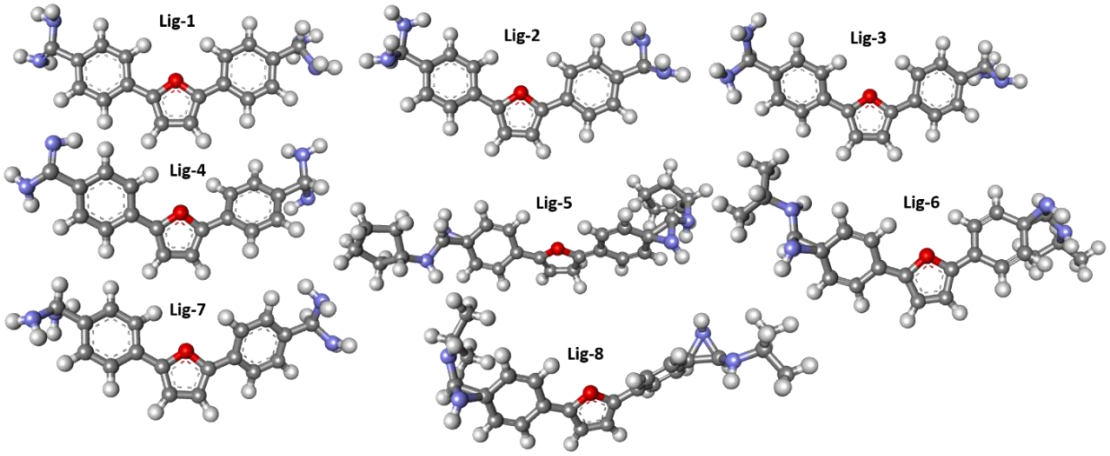

Figure 4: Optimized geometrical structures of class-1 of compounds

Table 1: DNA binding affinities of complexes for class-1 compounds

Substitution R	**Exp.** (ΔTm)	**1BNA** (kcal / mol)	**1DNE** (kcal / mol)	**1QSX** (kcal / mol)	**1RMX** (kcal / mol)	**195D** (kcal / mol)	**2MNB** (kcal / mol)	**2MNE** (kcal / mol)	**4AH0** (kcal / mol)
H	11.7	**-9.89**	**-13.45**	**-10.19**	**-10.69**	-10.88	-9.59	**-10.44**	-10.64
i-Pr	14.4	-8.60	-12.55	-9.71	-10.29	-10.03	**-9.74**	-9.54	**-11.36**
c-Pentyl	15.8	-9.42	-13.40	-10.12	-9.49	**-11.35**	-9.53	-9.83	-10.73
c-Pr	12.4	-7.60	-9.32	-6.29	-8.22	-7.58	-6.50	-6.36	-7.21
2-Pentyl	7.7	-7.60	-10.48	-9.04	-7.50	-9.44	-8.50	-7.38	-10.43

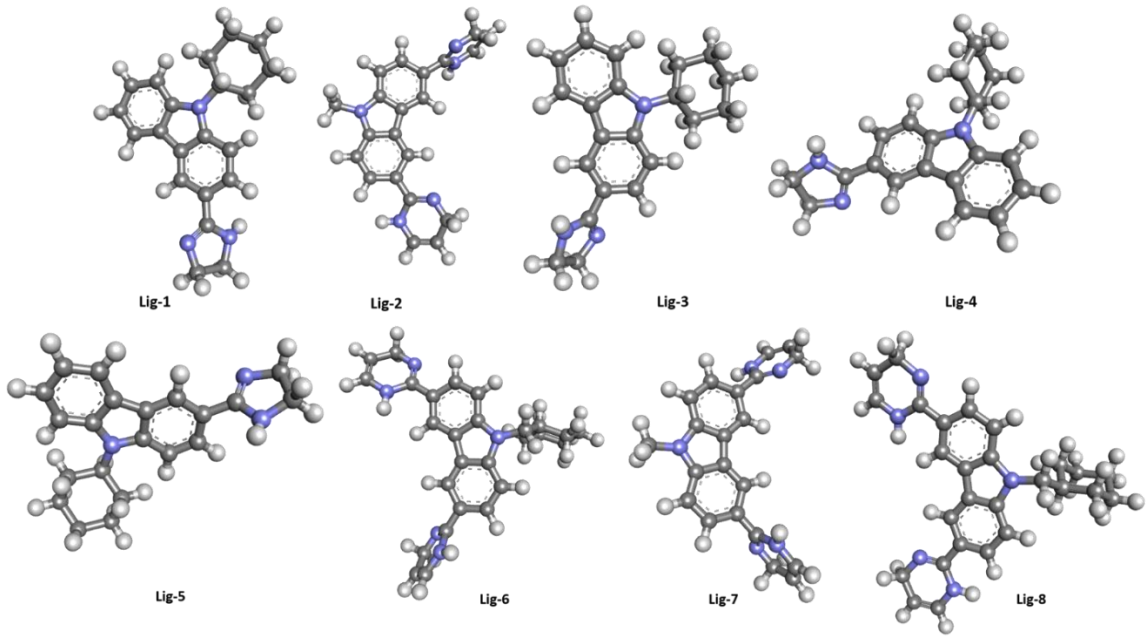

Figure 5: Optimized geometrical structures of class-2 of compounds

Table 2: DNA binding affinities of complexes for class-2 compounds

Substitutions				Exp. ΔT_m	1BNA	1DNE	1QSX	1RMX	195D	2MNB	2MNE	4AH0
R_1, R_2	**R_1**	**R_2**	**R_3**	**(°C)**	**(kcal/mol)**							
3,6	Am	Am	H	17.2	-7.51	-7.19	-6.81	-6.16	-7.90	-6.02	-6.98	-8.58
3,6	Am	Am	CH_3	19.5	-6.82	-7.24	-7.97	-6.00	-7.06	-6.23	-6.81	-6.63
2,6	IsoAm	IsoAm	H	9.6	-6.49	-7.41	-7.10	-6.86	-7.55	-6.05	-6.37	-9.02
3,6	Im	Im	H	19.5	-8.69	-7.92	-8.73	-5.96	-8.75	-7.35	-7.72	-9.20
3,6	Im	Im	CH_3	24.0	-7.72	-8.07	-8.27	-6.12	-8.54	-7.48	-7.57	-9.31
3,6	Im	H	CHM	16.8	**-9.75**	-8.47	**-9.78**	**-7.56**	**-9.86**	-7.11	-6.74	-9.66
3,6	THP	THP	CH_3	13.6	-8.58	**-8.89**	-8.67	-6.31	-8.92	-7.54	**-7.95**	-8.32
3,6	THP	THP	CHM	7.3	-8.78	-8.72	-6.57	-6.86	-9.78	**-7.72**	-7.54	**-10.24**
2,7	Am	Am	H	19.0	-7.21	-8.25	-7.97	-6.88	-8.37	-6.55	-6.65	-8.06
2,7	Im	Im	H	18.6	-8.25	-7.04	-9.11	-7.05	-9.05	-6.12	-6.04	-8.38
2,7	Im	Im	CH_3	19.1	-7.42	-8.84	-7.76	-6.12	-8.08	-6.50	-6.59	-8.02

It was observed from the analysis of obtained docking results that most of the drugs from both the class of ligands, were docked to the minor groove of the selected DNA sequences and their binding site was found to be AT-rich regions, as mostly preferred by DNA minor groove binders. Further, class-1 of the drugs are better DNA binders than class-2 of drugs, as the former has formed a greater number of hydrogen bonds than the later. The reason behind this is the geometry of the two class of compounds. This analysis will certainly help in improvement of the existing DNA minor groove binders having antimicrobial potency and would also prove helpful in the design of new and potent drugs and also it adds to the database regarding the structure activity relationship of ligands with DNA.

Chapter-4: Interaction, Dynamics and Stability Analysis of Some Minor Groove Binders with B-DNA Dodecamer 5'-(CGCAAATTTGCG)-3'

In this chapter, four molecules belonging to two different classes viz., 2,4-bis(4-amidinophenyl) furans and reversed diamidino 2,5-diarylfurans were selected and labelled as mol-1, mol-2 mol-3 & mol-4. Their geometry was optimized using Gaussian 09 at B3LYP/6-31G** level. The evaluation of relative binding strengths and stable complex formation tendencies with DNA (PDB Id: 4AH0) was performed in this chapter. Molecular docking was carried out using Autodock4 and molecular dynamics simulation was carried out using GROMACS software.

Figure 6 represents the optimized geometries of the selected drugs whereas **figure 7** illustrates the best docked posed complexes taken for molecular dynamics

simulations. Whereas **table 3** represents the variations in radius of gyration during the MD simulation. RMSD & RMSF analyses was performed to study the interaction dynamics in support of the stability of the predicted binding mode. **Figure 8** & **figure 9** represent the obtained RMSD & RMSF plots respectively.

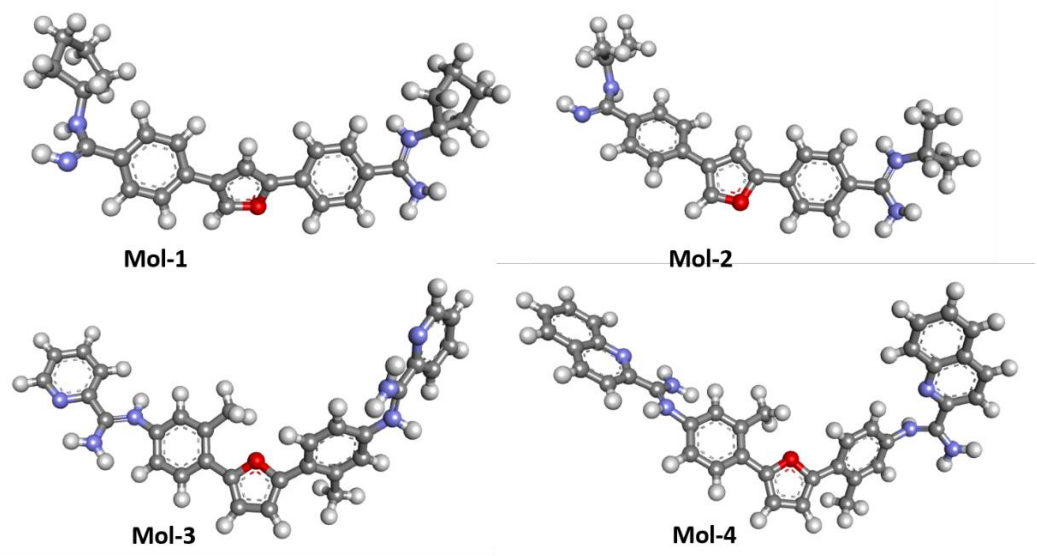

Figure 6: Figure showing optimized geometries of the selected ligands

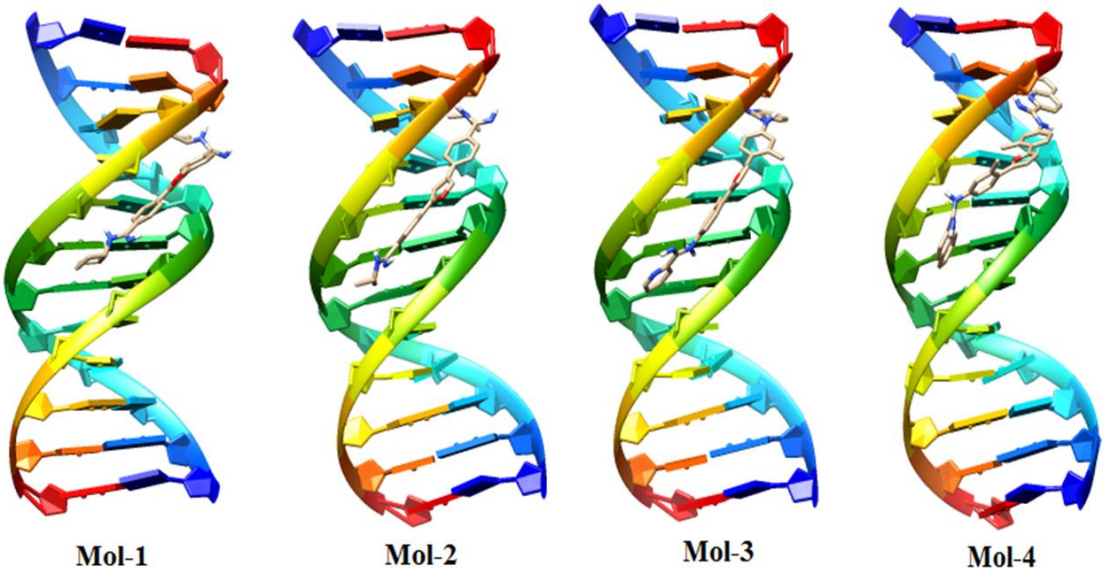

Figure 7: Figure showing best docked posed complexes

Table 3: Table summarizing the **v**ariation in radius of gyration for Drug-DNA Complexes

S. No.	Drug Molecule	4AH0 (avg. RG)
1.	Mol-1	Compact between 1.25nm to 1.50nm for first 3000ps, But between 3000~3500ps, 4000ps & 4500~5000ps there are several sharp fluctuations in the radii values **Remark:** non compact complex hence unstable
2.	Mol-2	Compact between 1.25nm to 1.50nm for entire 5000ps, **Remark:** Compact drug-DNA complex hence stable
3.	Mol-3	Compact between 1.25nm to 1.50nm for entire 5000ps, **Remark:** Compact drug-DNA complex hence stable
4.	Mol-4	Compact between 1.25nm to 1.50nm for entire 5000ps, **Remark:** Compact drug-DNA complex hence stable

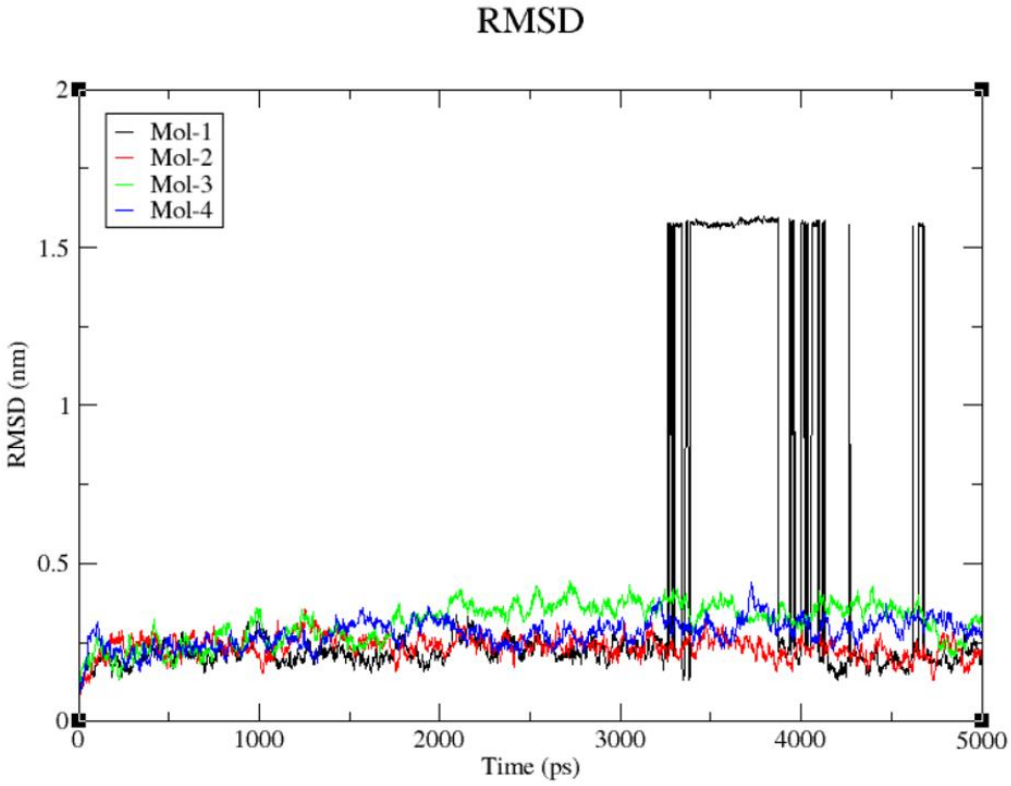

Figure 8: Figure representing RMSD for Drug-DNA Complexes

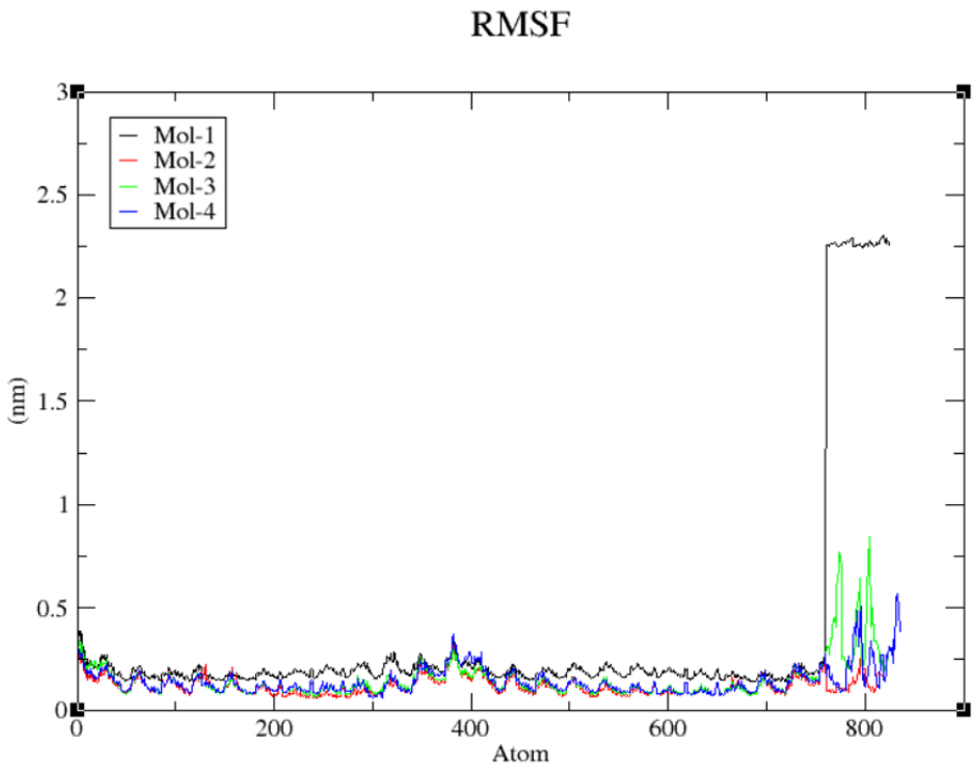

Figure 9: Figure representing RMSF for Drug-DNA Complexes

Docking results revealed that all the selected ligands were bound to the minor groove of the DNA. Their binding site was preferential AT-rich region. Also, the most stable complex as predicted by docking calculations was 4AH0 with mol-4 owing to the least docking binding energy of -12.39 kcal/mol. Results obtained from the molecular dynamics simulation show the time dependence of the stability of selected molecules in the vicinity of DNA. Radius of gyration, RMSD and RMSF analysis were done from the trajectories obtained via MD studies; all these results favor the stable complex formation for mol-2, mol-3 & mol-4 with 4AH0. Radius of gyration & RMSD values reveal that ligands remain bound to the preferred binding positions of the DNA without any considerable deviations in its minor groove; whereas the RMSF values reveal that the topological structure of DNA remains intact during the entire

course of the simulation, inferring the stability of drug-DNA complexes.

Obtained results not only predicted the conformational stability of the DNA with the ligands but also gave a firm affirmation regarding the time dependence of the interaction and stability of drug-DNA complexes. They also add strong affirmations regarding the benchmark of various computational techniques.

Chapter-5: Understanding Interactions of Some DNA Minor Groove Binders through Molecular Dynamics Simulations and MMPBSA Free Energy Calculations

In this chapter the recognition of 2 DNA-minor groove binding complexes (labelled, mol-1 & mol-2) in sequence-selective manner are presented using advanced *in silico* methods, which provides the basis for designing new drugs. Drugs were selected from literature, and crystal structures of the selected DNA sequences (PDB Ids: 1DNE & 195D) was downloaded from Protein Data Bank. The water molecules were removed from the crystal structure of DNA using UCSF Chimera.

The selected drug molecules were subjected to geometry optimization using Gaussian 09 at B3LYP/6-31G** level. Molecular docking was carried out using Autodock4 and molecular dynamics simulation was carried out using GROMACS software. Free energy calculations were carried out using the g_mmpbsa module.

The chemical structure of minor groove binders which were used for the further study is shown in **figure 10**. **Table 4** & **table 5** summarize the docking results whereas **figure 11** & **figure 12** represent the interaction profile for the best docked posed complexes.

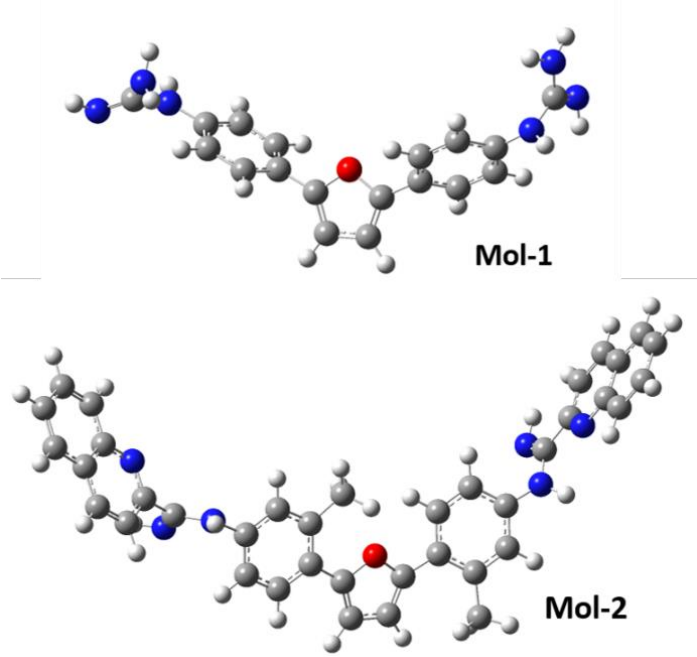

Figure 10: Figure showing optimized structures of the selected ligands

Table 4: Table representing docking results obtained for 1DNE sequence

S. No.	Molecule	Substitution		Exp. (ΔT_m)	1DNE				
		R	X	(°C)	Binding Free Energy (kcal/mol)	Inhibition Constant (nM)	Docking RMSD (Å)	No. of Conformers	Docking Temp. (K)
1.	mol-1	NHC(=NH)NH_2	H	10.8	-11.17	6.49	72.575	3	298.15
2.	mol-2	NHC(=NH)-2-Qu	CH_3	10.8	-13.54	119.86	83.548	1	298.15

*all energies are in kcal/mol

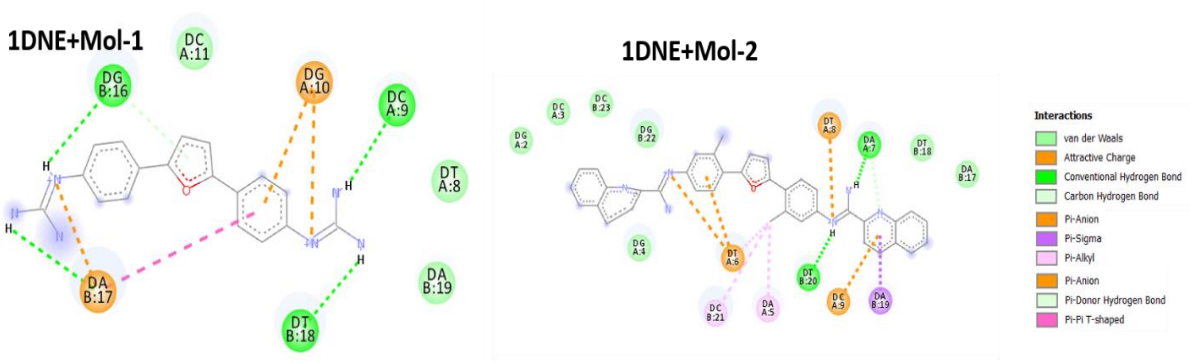

Figure 11: Figure representing interaction profile for the best docked posed complexes for 1DNE

Table 5: Table representing docking results obtained for 195D sequence

S. No.	Molecule	Substitution		Exp. (ΔT_m)	1DNE				
		R	X	(°C)	Binding Free Energy (kcal/mol)	Inhibition Constant (nM)	Docking RMSD (Å)	No. of Conformers	Docking Temp. (K)
1.	mol-1	$NHC(=NH)NH_2$	H	10.8	-11.38	4.52	25.643	2	298.15
2.	mol-2	NHC(=NH)-2-Qu	CH_3	10.8	-11.72	2.56	24.023	1	298.15

*all energies are in kcal/mol

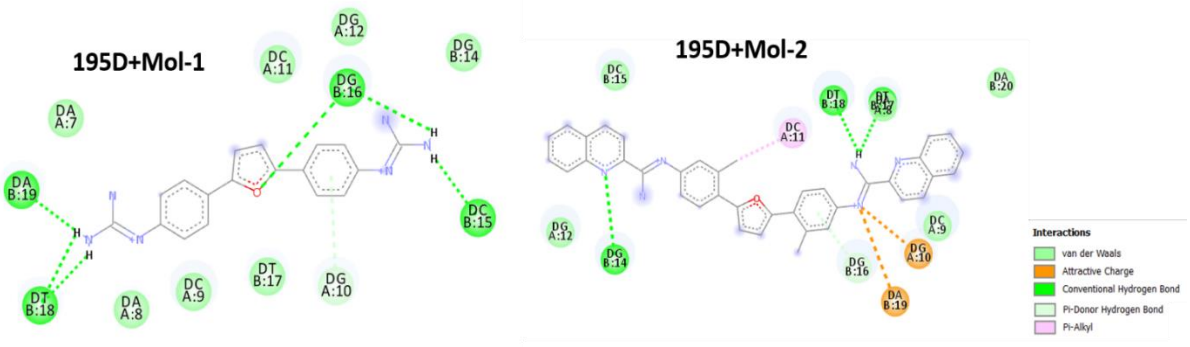

Figure 12: Figure representing interaction profile for the best docked posed complexes for 195D

Free energy calculations were performed followed by molecular dynamics simulations for gaining deep insights. Thermodynamic factors determining the stability of the formed complexes were obtained by MMPBSA calculations, whereas MD simulations briefed about the stability of the complexes. **Table 6** represents the variations in radius of gyration during the MD simulation. RMSD & RMSF analyses was performed to study the interaction dynamics in support of the stability of the predicted binding mode. **Figure 13** & **figure 14** represent the obtained RMSD & RMSF plots respectively. And **table 7** represents various energetic terms contributing towards the free energy of the complexes.

Table 6: Table summarizing the **v**ariation in radius of gyration for Drug-DNA Complexes

S. No.	**Drug Molecule**	**1DNE (avg. RG)**	**195D (avg. RG)**
1.	Mol-1	1.2nm, consistent throughout the simulation **Remark:** Compact DNA structure; Most stable complex	1.3nm~1.4nm, with numerous frequent sharp fluctuations **Remark:** unstable complex
2.	Mol-2	1.2nm, with sharp fluctuation at 2000ns, 4500ns and ~4750ns resp. **Remark:** Compact DNA structure; stable complex within 4500ns	1.275nm~1.425nm with numerous frequent sharp fluctuations **Remark:** unstable complex

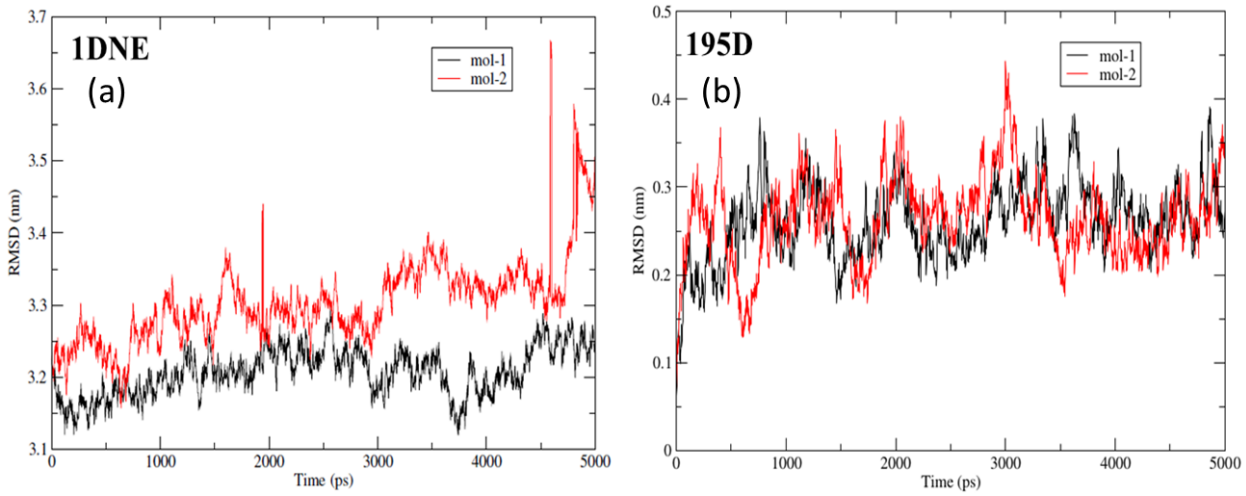

Figure 13: Figure representing RMSD for Drug-DNA Complexes

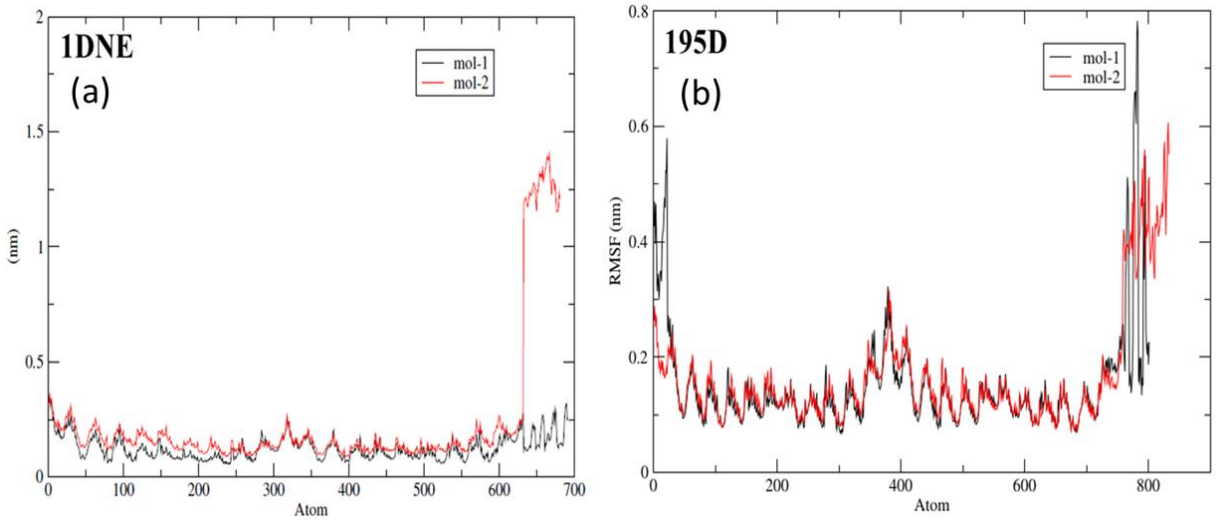

Figure 14: Figure representing RMSF for Drug-DNA Complexes

Table 7: Table representing the component-wise energy contributions for each drug-DNA pair

S. No.	Energy Term	1DNE		195D	
		Mol-1 (kJ/mol)	**Mol-2 (kJ/mol)**	**Mol-1 (kJ/mol)**	**Mol-2 (kJ/mol)**
1	Van der Waals energy	-97.318±9.428	-185.255±23.278	-66.352±31.113	-121.989±19.503
2	Electrostatic energy	-49.417±12.248	-44.114±17.444	-50.176±34.099	-33.822±25.373
3	Polar solvation energy	51.252±9.816	34.384±33.969	41.507±35.380	17.709±27.876
4	SASA energy	-10.254±0.829	-18.334±2.055	-7-719±2.810	-13.414±2.072
5	Binding energy	-105.736±17.243	-213.319±39.215	-82.740±37.767	-151.517±28.417

Molecular docking revealed stabilizing interactions because of the comparable binding affinities. However, since binding energy obtained for 1DNE+mol-2 is least this supports the stability of this complexes. It was also observed that all the ligands were minor groove binders and were docked to AT-rich sites of the DNA. Results obtained from MD simulation show the time dependence and the stability of selected molecules in the vicinity of DNA. The radius of gyration, RMSD & RMSF analyses reveal a stable complex formation for mol-1 & mol-2 with 1DNE. The results obtained by free energy calculations suggest that since binding energies for 195D is less than 1DNE, obtained through various contribution terms, so 195D has the most stable complex formation tendency than 1DNE.

This study describes the properties and dynamics of DNA on the interaction with selected molecules, taking the account of deformation upon binding which can play significant role in the discovery of new minor groove binder as a regulator of gene expression. Obtained results not only predicted the conformational stability of the DNA with the ligands but also gave a firm affirmation regarding the usage of computational techniques for studies of time dependence of the interaction and stability of drug-DNA complexes.

Chapter-6: Exploring Interactions of Some DNA Binding Ligands through Molecular Docking, Molecular Dynamics Simulations and Quantum Mechanical/Molecular Mechanical (QM/MM) Calculations

In this chapter two DNA-minor groove binders that were claimed to possess antimicrobial tendencies (labelled, lig-1 & lig-2) are selected for investigations of their DNA binding tendencies presented using advanced *in silico* methods. Drugs were selected from literature, and crystal structures of the selected DNA sequences (PDB Id: 1BNA) was downloaded from Protein Data Bank. The water molecules were removed from the crystal structure of DNA using UCSF Chimera.

The selected molecules were put to geometry optimization using Gaussian 09 at B3LYP/6-31G** level. Molecular docking was carried out using Autodock4 and molecular dynamics simulation was carried out using GROMACS software. DFT incorporated quantum mechanical/molecular mechanical (QM/MM) calculations were performed for the accurate determinations of the ligand binding affinities.

Figure 15 represents the optimized geometries of the selected drugs whereas **figure 16** illustrates the best docked posed complexes considered for molecular dynamics simulations. RMSD & RMSF analyses was performed to study the interaction dynamics in support of the stability of the predicted binding mode. **Figure 17** & **figure 18** represent the obtained RMSD & RMSF plots respectively.

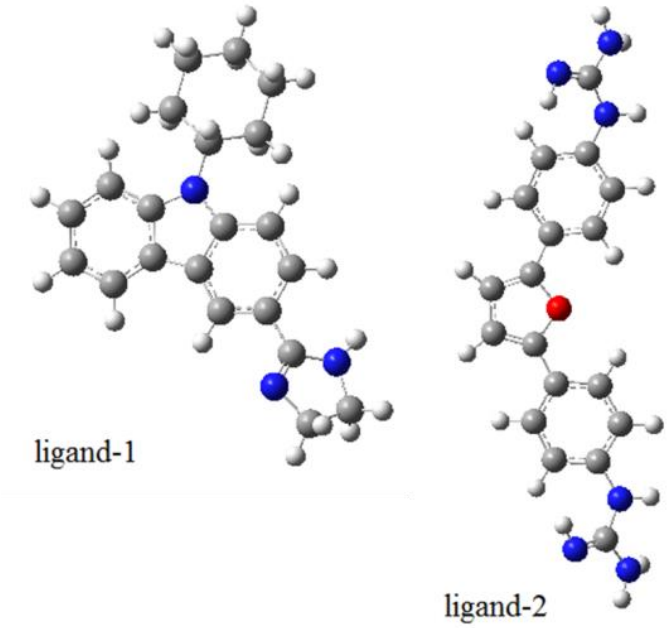

Figure 15: Figure showing optimized structures of the selected ligands

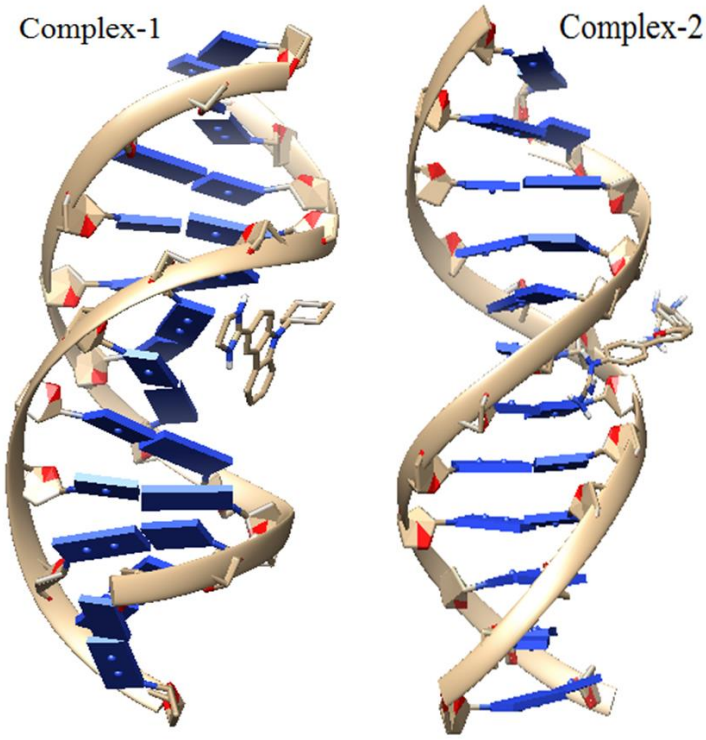

Figure 16: Figure showing best docked posed complexes for 1BNA

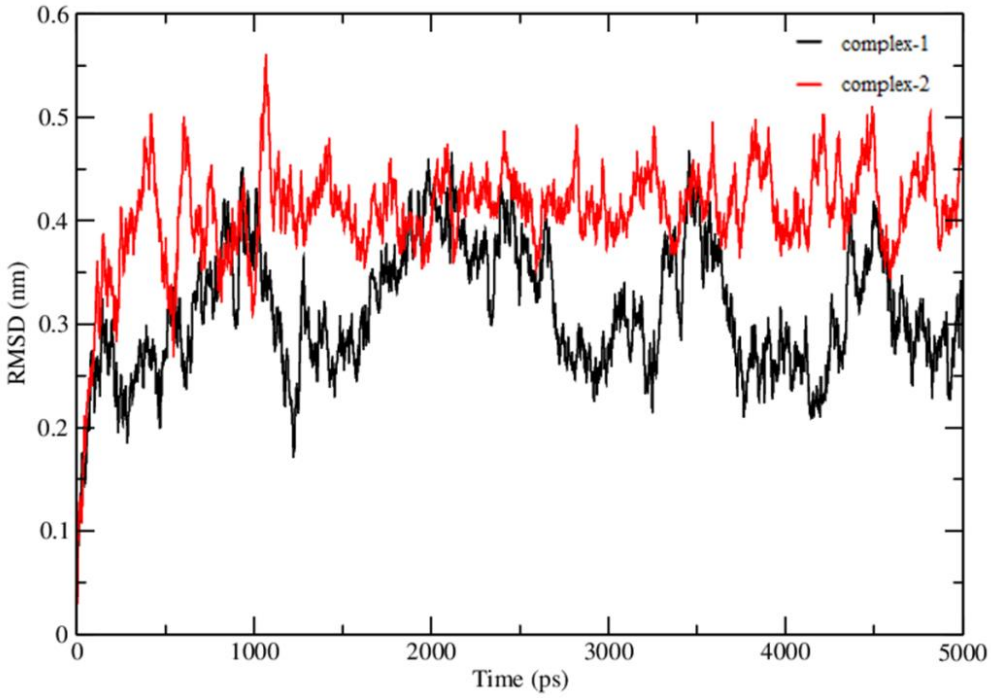

Figure 17: Figure representing RMSD for Drug-DNA Complexes

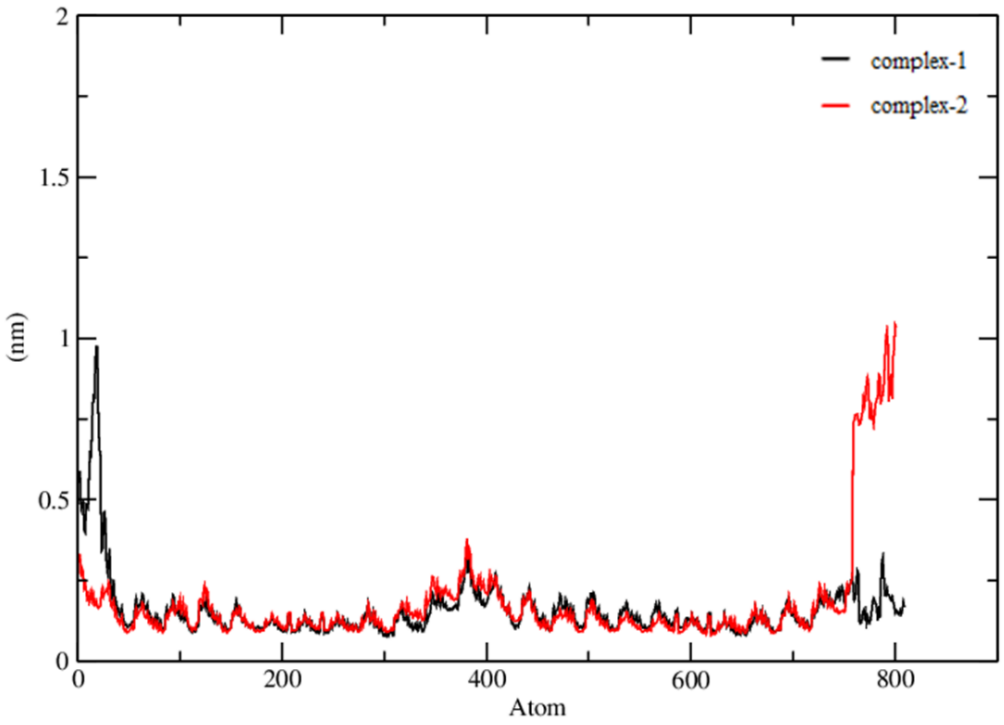

Figure 18: Figure representing RMSF for Drug-DNA Complexes

In this chapter, the quantum mechanical/molecular mechanical (QM/MM) calculations were performed using the two-level ONIOM method embedded within the Gaussian 09 program. B3LYP hybrid functional along with 6-31++G basis set was used for the higher layer (QM region of the system) whereas AMBER force field was incorporated for the lower layer (MM region of the system). The interaction energy between the DNA and drug molecule is calculated with the help of formula:

$$\Delta E_{IE} = E_{QM(gp)} - E_{QM(pp)} \quad (1)$$

Where, ΔE_{IE} is the interaction energy between drug and the DNA, $E_{QM(pp)}$ is the energy of QM region in nucleic acid phase and $E_{QM(gp)}$ is the energy of QM region in the gas phase.

Figure 19 represents one of the many snapshots taken from the MD results which acted as the basis for QM/MM calculations whereas **table 8** represents the obtained energies (ΔE_{IE}) through QM/MM calculations.

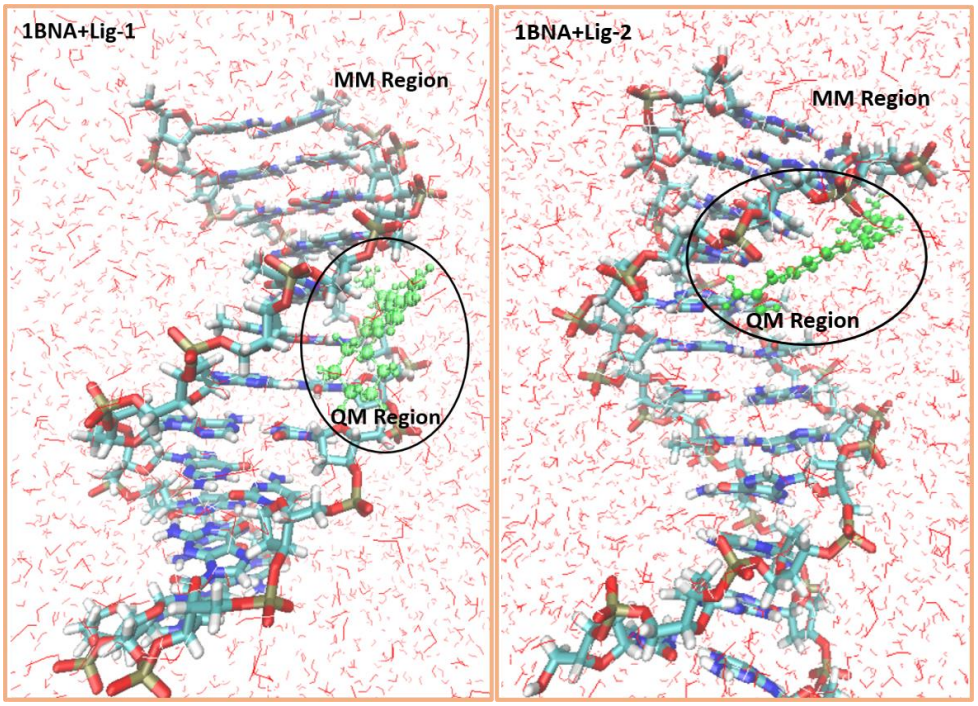

Figure 19: Figure representing one of the snapshots of DNA-ligand complexes

Table 8: Table showing the obtained energies (ΔE_{IE}) through QM/MM calculations

S. No.	Time Scale	Complex-1	Complex-2
		ΔE_{IE} (kcal/mol)	ΔE_{IE} (kcal/mol)
1	**1ns**	-1.733	-4.367
2	**2ns**	+2.902	-7.282
3	**3ns**	-1.714	-3.334
4	**4ns**	-1.300	-4.578
5	**5ns**	-2.125	-1.776

Docking results revealed that lig-1 was bound to major groove of the DNA whereas lig-2 was bound to minor groove of DNA. They were strictly bound to AT-rich regions of the DNA. Also, mol-2 had least binding energy of -10.69 kcal/mol. This claims to maximum stability of the formed complex between mol-2 and 1BNA. Molecular dynamics simulation shows the time evolution of the stability of ligands in the vicinity of DNA. Radius of gyration & RMSD values reveal that ligands remain bound to the preferred binding positions of the DNA without any considerable deviations RMSF analysis revealed that the topological structure of DNA remains intact during the entire course of the simulation, inferring the stability of drug-DNA complexes. QM/MM calculations were then carried out for better understanding of the results obtained through MD simulations. The results obtained suggest that since binding energies for lig-2 is less than lig-1, so complex-2 has the most stable complex. Because lig-2 did not offer any steric hindrances during the DFT studies and hence the repulsions between their nearest bonded atoms, between the angles and between corresponding dihedrals was minimized and the complex-2 attained an energy state having least bonded repulsions and therefore maximum stability was achieved and that state would correspond to minimum energy.

The results obtained through computational calculations not only predicted the conformational stability of the DNA with the ligands but also gave a firm affirmation regarding the time dependence of the interaction and stability of drug-DNA complexes. The extension of such studies involving computational techniques is not only limited to drug design and molecular modelling but also to drug metabolism.

Chapter-7: Conclusions

This chapter focuses upon the conclusions drawn from the investigations carried out on the computational studies of drug-DNA interactions in this thesis. It also provides the strategies for further research work in the field of drug discovery via computational advances. The concluding remarks made and the recommendations suggested for future works are as follows:

1. The focus of the study is to confirm the importance of DNA sequence and specificity in directing the complex formation at molecular levels. And our study attempts to give detail insight on the complexity in binding modes of small molecules to DNA.
2. Docking results were well explained through various series of analysis and thus were found to be in good co-relation with the results reported in the literature.
3. Dynamical behavior of the system was well studied and critical analysis of the in-depth information regarding the stability of the drug-DNA complex with evolving time was done by evaluating various parameters such as, variations in energy, variations in radii of gyrations, variations in number of hydrogen bonds, RMSD and RMSF.
4. The free energy calculations performed also added to the computational rigrousity of the calculations by incorporating the electrostatic effects and their exhaustiveness added to more detailed results, viz., energy contributions for each component (van der Waals energy, electrostatic energy, polar solvation energy, binding energy and SASA energy) and also per-residue contribution

was also obtained and hence critical analysis of the obtained results was achieved.

5. QM/MM calculations provide much better results than that of other molecular modeling methods such as molecular docking and molecular dynamics results owing to incorporation of DFT.
6. The use of MD simulations approach with QM/MM calculations allowed us to provide a theoretical protocol for complementing experimental techniques.
7. These collaborative computational modelling studies performed at electronic structure levels can give a great insight and add huge valuable information in designing novel inhibitors in close relationship with experimental works.

References:

[1] Avery, O.T., Maclend, C., Mc Carty, M., *The Journal of Experimental Medicine*, **79**,137-158 (1944).

[2] Chargaff, E., *J Cell Physiol. Suppl.*, **38**, 41-59 (1951).

[3] Franklin, R., and R. G. Gosling, R.G., *Nature*, **171**, 740–741 (1953).

[4] Watson, J.D., Crick, F.H.C., *Nature*, **171**, 737-738 (1953).

[5] Watson, J.D., Crick, F.H.C., *Nature*, **171**, 964-967 (1953).

[6] Dickerson, R.E., Drew, H.R., Conner, B.N., Wing, R.M., Fratini, A.V., Kopka, M.L., *Science*, **216,** 475-85 (1982).

[7] Gershell, L., Atkins, J., *Nature Reviews Drug Discovery*, **2**, 321–327 (2003).

[8] Gawehn, E., Hiss, J.A., Brown, J.B., Schneider, G., *Expert Opinion on Drug Discovery*, **13**, 579-582 (2018).

[9] Bahuguna, A., Rawat, D.S., *Med. Res. Rev.*, **40**, 263-292 (2020).

[10] Gaussian 09, Revision E.01, Frisch, M. J., Trucks, G. W., Schlegel, H. B.; Scuseria, G. E., Robb, M. A., Cheeseman, J. R., Scalmani, G., Barone, V., Mennucci, B., Petersson, G. A., Nakatsuji, H., Caricato, M., Li, X., Hratchian, H. P., Izmaylov, A. F., Bloino, J., Zheng, G., Sonnenberg, J. L., Hada, M., Ehara, M., Toyota, K., Fukuda, R., Hasegawa, J., Ishida, M., Nakajima, T., Honda, Y., Kitao, O., Nakai, H., Vreven, T., Montgomery, J. A., Jr., Peralta, J. E., Ogliaro, F., Bearpark, M., Heyd, J. J., Brothers, E., Kudin, K. N., Staroverov, V. N., Kobayashi, R., Normand, J., Raghavachari, K., Rendell, A., Burant, J. C., Iyengar, S. S., Tomasi, J., Cossi, M., Rega, N., Millam, J. M., Klene, M., Knox, J. E., Cross, J. B., Bakken, V., Adamo, C., Jaramillo, J., Gomperts, R., Stratmann, R. E., Yazyev, O., Austin, A. J., Cammi, R., Pomelli, C., Ochterski, J. W., Martin, R. L., Morokuma, K., Zakrzewski, V. G., Voth, G. A., Salvador, P., Dannenberg, J. J., Dapprich, S., Daniels, A. D., Farkas, Ö., Foresman, J. B., Ortiz, J. V., Cioslowski, J., Fox, D. J. Gaussian, Inc., Wallingford CT, 2009.

[11] Morris, G.M., Huey, R., Lindstrom, W., Sanner, M.F., Belew, R.K., Goodsell, D.S., Olson, A.J., *Journal of Computational Chemistry*, **30**, 2785–2791 (2009).

[12] Pettersen, E.F., Goddard, T.D., Huang, C.C., Couch, G.S., Greenblatt, D.M., Meng, E.M., Ferrin, T.E., *Journal of Computational Chemistry*, **25**, 1605-1612 (2004).

[13] Dassault Systèmes BIOVIA, *Discovery Studio* Modeling Environment, San Diego (2020).

[14] Humphrey, W., Dalke, A., Schulten, K., *J. Molec. Graphics*, **14**, 33-38 (1996).

[15] Turner, P.J., XMGRACE, Version 5.1. 19. Center for Coastal and Land-Margin Research, Oregon Graduate Institute of Science and Technology, Beaverton, OR (2005).

[16] Abraham, M.J., Murtola, T., Schulz, R., Pall, S., Smith, J.C., Hess, B., Lindahl, E., *SoftwareX*, **1–2**, 19–25 (2015).

[17] Kumari, R., Kumar, R., Lynn, A., *Journal of Chemical Information and Modeling*, **54**, 1951-1962 (2014).

[18] Braun, E., Gilmer, J., Mayes, H.B., Mobley, D.L., Jacob, I., Prasad, S., Zuckerman, D.M., **1**, 1–28 (2019).

[19] Kollman, P.A., Massova, I., Reyes, C., Kuhn, B., Huo, S., Chong, L., Lee, M., Lee, T., Duan, Y., Wang, W., Donini, O., Cieplak, P., Srinivasan, J., Case, D.A., Cheatham, T.E., *Accounts of Chemical Research*, **33,** 889-897 (2000).

[20] Genheden, S., Ryde, U., *Expert Opinion on Drug Discovery*, **10**, 449-46 (2015).

[21] Zoete, V., Cuendet, M.A., Grosdidier, A., Michielin, O., *Journal of Computational Chemistry*, **32**, 2359-2368 (2011).

[22] Mark, P., Nilsson, L., *Journal Physical Chemistry-A,* **105,** 9954-9960 (2001).

[23] Hess, B., Bekker, H., Berendsen, H.J.C., Fraaije, J.G.E.M., *Journal of Computational Chemistry*, **18**, 1463-1472 (1997).

[24] Zhao, H., Caflisch, A., *European Journal of Medicinal Chemistry*, **94**, 4-14 (2015).

[25] da Silva, A.W. S., Vranken, W.F., *BMC Res. Notes*, **5**, 367 (2012).